NJC

Accepted Manuscript

This article can be cited before page numbers have been issued, to do this please use: R. Ratha, M. A. Afroz, R. K. Gupta and P. K. Iyer, *New J. Chem.*, 2019, DOI: 10.1039/C8NJ05850D.

Volume 40 | Number 1 | January 2016 | Pages 1–846

NJC

New Journal of Chemistry
www.rsc.org/njc

A journal for new directions in chemistry

ISSN 1144-0546

ROYAL SOCIETY OF CHEMISTRY

PAPER
Jaison B. Benedict et al
The role of atropisomers on the photo-reactivity and fatigue of diarylethene-based metal–organic frameworks

View Article Online
DOI: 10.1039/C8NJ05850D

NJC

PAPER

Received 00th January 20xx,
Accepted 00th January 20xx

DOI: 10.1039/x0xx00000x

www.rsc.org/

Substituting non-conjugating ester group on benzothiadiazole side chain in donor-acceptor polymer improves the solar cell performance

Radhakrishna Ratha,[a] Mohammad Adil Afroz,[b] Ritesh Kant Gupta[a] and Parameswar Krishnan Iyer*[a,b]

Herein, the effect of non-conjugated ester functionalization at 5,6-position of 2,1,3-benzothiadiazole (BT) in donor (D)-acceptor (A) conjugated polymer (CP) used for photovoltaic devices have been investigated. Position 5 and 6 of BT have been functionalized with methyl acetate group and its structure property relationship have been compared with BT having methyl group at 5,6-positions in four types of D-A CPs. Alternate co-polymers of newly synthesized methyl and methyl acetate derivatives of BT and Th-BT-Th with commonly used donors such as dithiophene (DTh) and benzodithiophene (BDT) have been synthesized using Stille coupling reaction namely P(1,2,3,4)-Me and P(1,2,3,4)-Ac. All CPs have been extensively characterized by GPC, UV-visible, ^{1}H-NMR, ^{13}C-NMR, TGA and CV. Optimized geometry along with change of dihedral angle on substitution of acetate group have been analysed by density functional theory (DFT) by B3LYP/6-31G (*d,p*). The side chain ester group lowers the dihedral angle, improves optical and electrochemical properties of CPs used for PSC, improves phase separation of active layer and performance of the fabricated PSC compared to its methyl counterpart, as investigated for P(1,2,3,4)-Me and P(1,2,3,4)-Ac. On fabrication of BHJ solar cell with geometry of device as ITO/PEDOT:PSS/P-PC$_{71}$BM/LiF/Al, CP having methyl acetate functionalization such as P2-Ac, P3-Ac and P4-Ac resulted in higher PCE of 1.36%, 1.17% and 0.35% compared to their methyl counterpart CP P2-Me, P3-Me and P4-Me with PCE of 0.9%, 0.54% and 0.31% respectively. With 1,8-diiodooctane (DIO) as additive, higher PCE of 1.96% was achieved from P3-Ac as well. Atomic force microscopy (AFM) and thin film X-ray diffraction (XRD) have been used to determine the impact of side chain ester group on π-π stacking distance among CP main chain in film state and morphology of active layer of fabricated PSCs respectively.

Introduction

Harvesting solar energy using a blend of donor(D)-acceptor(A) containing p-type conjugated polymer (CP) donors and n-type fullerene / non-fullerene-based acceptor in a bulk-heterojunction[1] inverted[2] / ternary[3,4,5] / tandem[6] geometry polymer solar cells (PSCs), is approaching a power conversion efficiency (PCE) close to 11-13%[1,7] and durability of the order of 7 years.[8] Besides designing several acceptors (fullerene/ non-fullerene)[9] and device engineering, the journey to a PCE of >11% was viable during last 10-15 years due to the large number of CPs having desired properties such as, (i) absorption maximum in 700-800 nm region of solar spectrum with molar absorption coefficient of the order of $5*10^3$ L mol^{-1} cm^{-1}, (ii) hole mobility of the order $1*10^2$ cm^2 V^{-1} s^{-1}, (iii) having suitably positioned HOMO and LUMO corresponding to n-type acceptor used for blending during fabrication. To further increase the PCE and establish in-depth structure property relationship, design of new backbones and modification of old ones are necessary. Though the major focus among the modifications have been on donor CP main chain,[10,11] various research groups have also functionalized the side chain of these CPs such as: phosphite functionalized side chain CP (used as electron transporting layer[12] and additional interlayer),[13,14] side chain cyanide substituted CP (reported to have improve dielectric constant),[15] azide substituted CP (to improve crosslinking property)[16] and incorporation of functional group to enhance the solubility.[17]

Moreover, significant efforts have also been given to improve the active layer morphology to enhance the charge separation and to reduce the recombination of generated exciton. An optimized active layer (polymer-PCBM/non-fullerene) morphology of a PSC device should: be less aggregated,[18,19] orderly arranged/crystalline film with bi-continuous phase[20-22] and having least RMS roughness with small grain size.[23] These preferred morphological variations have been achieved majorly by; (i) use of additives[24,25]/mixture of solvents[13] /

---

[a] Centre for Nanotechnology, Indian Institute of Technology Guwahati, Guwahati-781039, Assam, INDIA, Email: pki@iitg.ac.in

[b] Department of Chemistry, Indian Institute of Technology Guwahati, Guwahati-781039, Assam, INDIA.

† Electronic Supplementary Information (ESI) available: [materials, methods, solar cell fabrication procedure, ^{1}H-NMR, ^{13}C-NMR, GPC and TXRD figures]. See DOI: 10.1039/x0xx00000x

View Article Online
DOI: 10.1039/C8NJ05850D

solvents to enhance solubility of the active layer,[26] as preferential solubility of PCBM in one solvent over other allows stepwise deposition of blend layer sequentially providing appropriate phase separation in the active layer allowing distinct path for transport of holes and electrons; and (ii) high temperature annealing[27] during device fabrication, providing sufficient energy for the film to be well organized or upside down solvent vapour annealing.[28] In addition, incorporation of few functional group viz. fluorine / oxygen / nitrogen into CP backbone has also been shown as a proficient approach to improve morphology as well.[29-31]

In line with the discussion of designing CPs as solar harvester with good photo-physical property, mobility and having functional group which improves morphology of active layer, it is worth mentioning that CPs with main/side chain substituted functional groups such as fluorine, oxygen, sulphur, ester, ketone, cyanide and azide[10,16,32-35] are often being synthesized to improve solar cell performances. Such functional groups lower dihedral angle within CPs and bring planarity and linearity into it,[11] leading to improved π-π stacking in film state with desired morphology.[36] The reason for improvement of PSC performance in case of main chain/side chain functionalized CPs are enhanced intra-molecular/inter-molecular oxygen-sulphur (O-S)/fluorine-hydrogen (F-H) / nitrogen(N)-hydrogen(H)/oxygen-hydrogen (O-H) interaction of CP chains in film state.[37,16,38,39] This improves optical property in film state and segregation between CP and PCBM (acceptor), for the reason of enhanced interaction within polymer-polymer chain, which repels the PCBM and gives the most anticipated morphology called segregation rather than undesired morphology called aggregation.

Ester group is one such important functional group among all, being used both in the side chain and main chain of CPs for solar cell. It has been reported that ester group improves thermal stability of fabricated devices due to cross linking property,[40,41] thermo cleavable nature of ester group helps the active layer of PSC resistant to solvent during multilayer device fabrication,[42] impart promising solubility, along with mobility[43] and improves morphology of active layer in PSC as well.[44]

In this approach BT has been modified to improve the design and synthesize acceptor units with methyl acetate group substituted as side chain at 5,6-position of BT (Fig. 1). Synthesis of D-A kind of CPs have been carried out (namely P1-Ac, P2-Ac, P3-Ac, P4-Ac) from corresponding ester functionalized BT-based acceptors with commonly used donors (D1, D2, D3 and D4, Fig. 2) using Stille coupling. Corresponding methyl counterpart CPs (namely P1-Me, P2-Me, P3-Me and P4-Me) have also been synthesized to compare influence of ester group at 5,6-position of BT. Herein, it has been established that side chain ester group at 5,6-position of BT, (i) can lower the dihedral angle along the conjugation main chain resulting in increase in the molar absorption coefficient (ii) red-shift in the absorption spectra in film state (iii) lowers optical LUMO level due to electron withdrawing nature and (iv) enhances the solar cell performance of CP compared to its methyl counterpart. These enhanced property of side chain ester groups are due to oxygen-sulphur (O-S)/π-π and CH-π interactions both within the CP chain and/or inter-molecularly in film state of CP and/or CP-PCBM blend.

Experimental

Detailed stepwise synthesis scheme of monomers and polymers have been given in Fig. 1 and Fig. 2 respectively.

Synthetic procedures

5,6-Dimethyl-benzo[1,2,5]thiadiazole (2). Monomer **2** was prepared as per the literature procedure.[45]

4,7-Dibromo-5,6-dimethylbenzo[c][1,2,5]thiadiazole (3). Monomer **2** (0.5g, 1.55 mmol) and concentrated HBr (48 wt% ca. 30 mL) was added to a double neck reaction flask, connected with a condenser at one neck. The flask was fitted with an addition funnel at other neck to which Br_2 (0.470 mL, 9.134 mmol) solution in concentrated HBr (ca. 15 mL) was added slowly (2-3 drops per second) while stirring at room temperature. After few drops of addition the solution turns orange and a precipitate appears. After completion of addition the suspension was refluxed for 6 hours at 130 ^{o}C. To the suspension, excess amount of H_2O was added to quench excess of bromine present. It was then filtered, washed with H_2O repeatedly to give crude product, which upon further purification by chromatographic column (SiO_2, 50% $CHCl_3$ in hexane) yielded 75% cream coloured solid **3**. ^{1}H-NMR (400 MHz, $CDCl_3$, δ in ppm): 2.672 (s, 6H). ^{13}C-NMR (150 MHz, $CDCl_3$, δ in ppm): 152.12, 140.61, 114.68, 22.03. HR-MS: m/z $[M+H]^+$ calcd for $C_8H_6Br_2N_2S$ 322.868, found 322.868.

4,7-Dibromo-5,6-bis(bromomethyl)benzo[c][1,2,5]thiadiazole (4). Monomer **4** was synthesized following free radical bromination procedure as per literature procedure[45] using 4,7-Dibromo-5,6-dimethylbenzo[c][1,2,5]thiadiazole **3** (0.5 g, 1.553 mmol), NBS (0.683 g, 3.883 mmol), benzoyl peroxide (0.037 g, 0.155 mmol) and 30 mL CCl_4. After chromatographic purification (SiO_2, 50% $CHCl_3$ in hexane) of crude product, gave compound **4** (cream coloured solid) with a yield of 92%.

4,7-Dibromobenzo[c][1,2,5]thiadiazole-5,6-diyl)bis(methylene) diacetate (5). Monomer **4** 0.9 g (1.87 mmol) and anhydrous NaOAc 2.55 g (5.6 mmol) was mixed inside a round bottom flask containing 25 mL of glacial ethanoic acid and refluxed overnight at 120 ^{o}C. The suspension was transferred into H_2O and neutralized with sodium bicarbonate solution in water. It was followed by work up with $CHCl_3$ and water. The organic portion was dried and desired product was separated with column chromatography using eluent (10% ethyl acetate in hexane) to get **5** (0.75 g, yield = 91.7%) as white colored solid. ^{1}H-NMR (600 MHz, $CDCl_3$, δ in ppm): 5.58 (s, 4H), 2.1 (s, 6H). ^{13}C-NMR (150 MHz, $CDCl_3$, δ in ppm): 170.44, 152.88, 137.28, 118.01, 63.83, 20.84. HRMS (ESI): m/z $[M+H]^+$ calcd for $C_{12}H_{10}Br_2N_2O_4S$ 438.878, found 439.215.

4,7-Di(thiophen-2-yl)benzo[c][1,2,5]thiadiazole-5,6-diyl)bis (methylene) diacetate (6). To a 50 ml flask monomer **5** (0.3 g 0.687 mmol), tributyl(thiophen-2-yl)stannane 0.77 g (2.06 mmol) and 25 mL of dry toluene was transferred. The flask was

View Article Online
DOI: 10.1039/C8NJ05850D

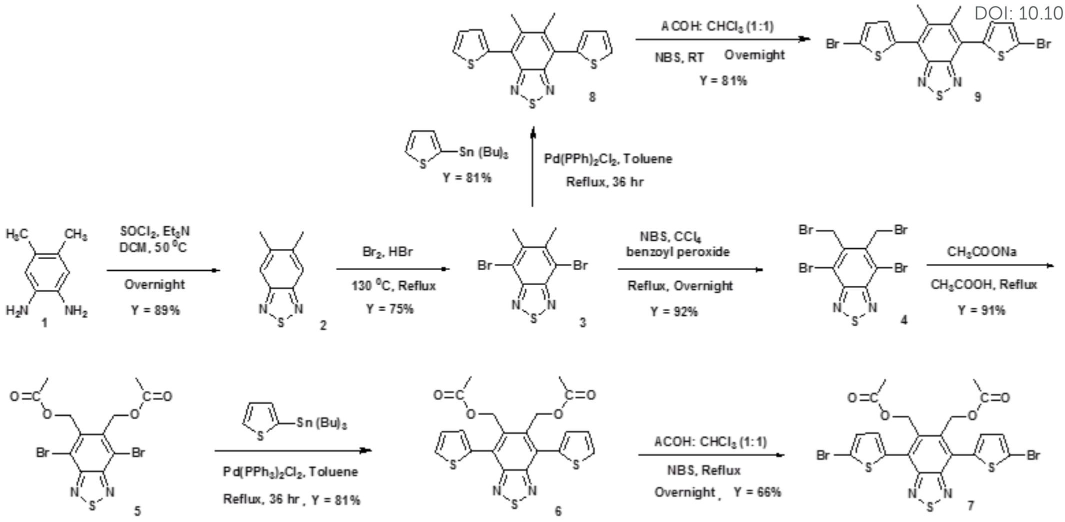

Fig. 1 Reaction scheme for synthesis of monomers.

purged for 5 minutes with argon before adding $Pd(PPh_3)_2Cl_2$ 0.024 g (0.034 mmol). It was then refluxed at 100 °C for 40 hours under argon flow. After cooling to RT, solvent was evaporated in rotary evaporator, and purified with column chromatography (5% ethyl ethanoate in hexane), to get 0.25 g of greenish yellow colored product **(6)** with 81% yield. ^{1}H-NMR (600 MHz, $CDCl_3$, δ in ppm): 7.61-7.60 (d, 2H), 7.31-7.30 (d, 2H), 7.26-7.23 (dd, 2H), 5.30 (s, 4H), 2.13 (s, 6H). ^{13}C-NMR (75 MHz, $CDCl_3$, δ in ppm): 170.15, 154.39, 135.03, 134.80, 130.08, 129.77, 128.16, 127.16, 61.81, 20.91. HRMS (ESI): m/z $[M+H]^+$ calcd for $C_{20}H_{16}N_2O_4S_3$ 445.038, found 445.0336.

4,7-Bis(5-bromothiophen-2-yl)benzo[c][1,2,5]thiadiazole-5,6-diyl)bis(methylene) diacetate (7). Inside a round bottom flask, monomer **6** (0.1 g, 0.22 mmol) was dissolved in $CHCl_3$: glacial acetic acid (1:1) and NBS (0.12 g, 0.675 mmol) was poured to it in one portion. It was refluxed overnight in dark and then evaporated to get crude product. Further column chromatographic (SiO_2, eluent 5% EtOAc in hexane) purification of the crude gave 0.09 g of monomer **7** (yellow colored solid, 66% yield). ^{1}H-NMR (600 MHz, $CDCl_3$, δ in ppm): 7.19-7.18 (d, 2H), 7.06-7.05 (d, 2H), 5.30 (s, 4H), 2.13 (s, 6H). ^{13}C-NMR (75 MHz, $CDCl_3$, δ in ppm): 170.10, 154.02, 136.31, 135.28, 130.25, 130.12, 129.40, 115.54, 61.65, 20.94. HRMS (ESI): m/z $[M+H]^+$ calcd for $C_{20}H_{14}Br_2N_2O_4S_3$ 602.858, found 602.858.

5,6-Dimethyl-4,7-di(thiophen-2-yl)benzo[c][1,2,5]thiadiazole (8). Synthesis of monomer **8** was performed as like monomer **6,** by using monomer **3** (0.4 g, 1.24 mmol), tributyl(thiophen-2-yl) stannane (1.39 g 3.7 mmol) and $Pd(PPh_3)_2Cl_2$ (0.043 g, 0.0621 mmol). The product was separated from the mixture by doing silica gel column chromatography (with eluent 15% $CHCl_3$ in hexane) to give 0.33 g of compound **8** as greenish yellow coloured solid (yield = 81%). ^{1}H-NMR (600 MHz, $CDCl_3$, δ in ppm): 7.56-7.55 (d, 2H), 7.24-7.23 (dd, 2H), 7.129-7.123 (d, 2H), 2.48 (s, 6H). ^{13}C-NMR (75 MHz, $CDCl_3$, δ in ppm): 153.79, 139.78, 137.41, 128.74, 127.04, 126.79, 125.50, 18.99. HRMS (ESI): m/z $[M+H]^+$ calcd for $C_{16}H_{12}N_2S_3$ 329.028, found 329.024.

4,7-Bis(5-bromothiophen-2-yl)-5,6-dimethylbenzo[c][1,2,5]thiadiazole (9). Following the procedure used to synthesize monomer **7**, Monomer **9** was synthesized by taking monomer **8** (0.25 g, 0.75 mmol) and NBS (0.4 g, 2.28 mmol) with room temperature stirring in dark. 10% $CHCl_3$ in hexane as eluent was used in column chromatography to yield pure monomer **9** as yellow coloured solid (0.3 g, 81% yield). ^{1}H-NMR (600 MHz, $CDCl_3$, δ in ppm): 7.182-7.76 (d, 2H), 6.954-6.948 (d, 2H), 2.50 (s, 6H). ^{13}C-NMR (75 MHz, $CDCl_3$, δ in ppm): 153.34, 140.02, 138.79, 129.90, 129.26, 124.92, 113.71, 19.01. HRMS (ESI): m/z $[M+H]^+$ calcd for $C_{16}H_{10}Br_2N_2S_3$ 486.848, found 486.846.

General synthetic methodology for polymerization using Stille coupling. Donor monomer **(D1/D2/D3/D4)** and acceptor monomer **(3/5/7/9)** in equivalents of 1:1 were taken into a 50 mL reaction flask and 25 mL of dry toluene was added to it. Before addition of 0.2 equivalent of $Pd(PPh_3)_4$, it was purged with argon for 5 minutes. It was then degassed and purged with argon thrice. It was then refluxed at 100 °C for 72 hours in presence of Ar. After reducing the temperature to 25 °C, the crude was concentrated and precipitated into 400 ml of methyl alcohol. The precipitates were collected washed with MeOH, dried and then dissolved in chloroform. The solution was filtered twice to remove insoluble part, concentrated and again precipitated with 300 mL of methyl alcohol.

View Article Online
DOI: 10.1039/C8NJ05850D

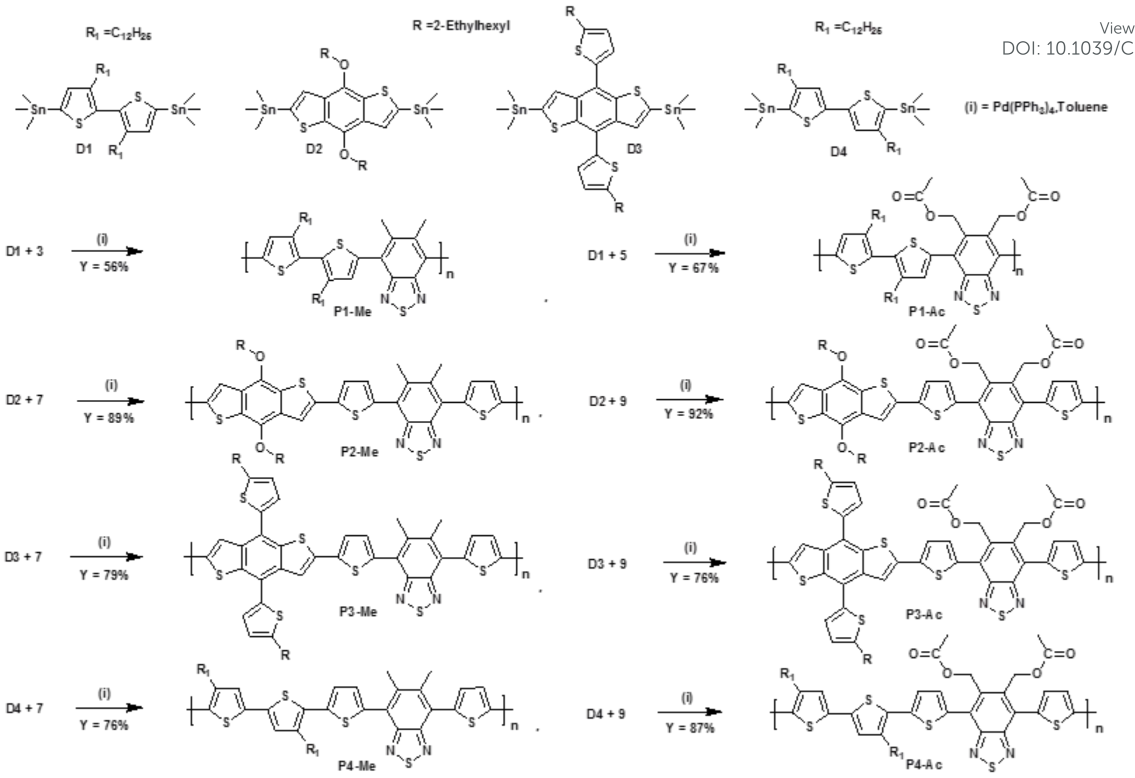

Fig. 2 Reaction scheme for synthesis of CPs.

The precipitates were carefully collected to get desired CP.

P1-Me. It was synthesized using monomer **D1** (0.1 g, 0.1207 mmol), monomer **3** (0.038 g, 0.1207 mmol) and Pd(PPh$_3$)$_4$ (14 mg, 0.02414 mmol). P1-Me was formed as yellow colored sticky solid (45 mg, yield 56%). ^{1}H-NMR (600 MHz, CDCl$_3$, δ in ppm): 7.14-7.12 (br, 1H), 7.09-7.07 (br, 1H), 2.71-2.69 (br, 2H), 2.62-2.55 (br, 6H), 1.78-1.68 (br, 4H), 1.43-1.38 (br, 2H), 1.26-1.25 (br. 36H), 0.88-0.86 (br, 6H). GPC: M_n = 12600 g/mol.; M_w = 15883 g/mol.; PDI = 1.26; degree of polymerization, n = 16.

P1-Ac. It was synthesized using monomer **D1** (0.1 g, 0.1207 mmol), monomer **5** (0.0526 g, 0.1207 mmol) and Pd(PPh$_3$)$_4$ (27.8 mg, 0.02414 mmol). P1-Ac was formed as reddish yellow colored powder (60 mg, yield 67.3%). ^{1}H-NMR (600 MHz, CDCl$_3$, δ in ppm): 7.26-7.25 (br, 1H), 7.20-7.17 (br, 1H), 5.39 (br, 4H), 2.78-2.68 (br, 2H), 2.23-1.98 (br, 6H), 1.74-1.62 (br, 4H), 1.44-1.37 (br, 2H), 1.37-1.12 (br, 36H), 0.91-0.80 (br, 6H). GPC: M_n = 4986 g/mol.; M_w = 5396 g/mol.; PDI = 1.08; degree of polymerization, n = 7.

P2-Me. It was synthesized using monomer **D2** (0.07 g, 0.09042 mmol), monomer **7** (0.04385 g, 0.09042 mmol) and Pd(PPh$_3$)$_4$ (20.8 mg, 0.018 mmol). P2-Me was formed as red colored powder (62 mg, yield 89%). ^{1}H-NMR (600 MHz, CDCl$_3$, δ in ppm): 7.69-7.66 (br, 1H), 7.63-7.59 (br, 1H), 7.51-7.46 (br, 2H), 7.26-7.20 (br, 2H), 4.31-4.23 (br, 4H), 2.67-2.58 (br, 6H), 1.95-1.83 (br, 2H), 1.62-1.54 (br, 4H), 1.53-1.39 (br, 12H), 1.16-0.94 (br, 12H). GPC: M_n = 11580 g/mol.; M_w = 15300 g/mol.; PDI = 1.29; degree of polymerization, n = 15.

P2-Ac. It was synthesized using monomer **D2** (0.07 g, 0.09042 mmol), monomer **9** (0.0544 g, 0.09042 mmol) and Pd(PPh$_3$)$_4$ (20.8 mg, 0.018 mmol). P2-Ac was formed as deep red colored solid (74 mg, yield 92%). ^{1}H-NMR (600 MHz, CDCl$_3$, δ in ppm): 7.71-7.65 (br, 1H), 7.60-7.51 (br, 1H), 7.45-7.36 (br, 2H), 7.30-7.28 (br, 2H), 5.48-5.39 (br, 4H), 4.32-4.21 (br, 4H), 2.24-2.15 (br, 6H), 1.95-1.85 (br, 2H), 1.64-1.53 (br, 4H), 1.53-1.40 (br, 12H), 1.16-1.09 (br, 12H). ^{13}C-NMR (150 MHz, CDCl$_3$, δ in ppm): 170.18, 154.16, 144.5, 144.33, 140.55, 136.07, 135.31, 135.21, 132.54, 130.99, 130.17, 129.73, 129.46, 125.28, 124.54, 118.25, 116.79, 114.09, 76.24, 62.0, 40.64, 31.94, 30.46, 29.23, 23.99, 20.99, 14.21, 11.37. GPC: M_n = 11581, g/mol.; M_w = 11959 g/mol.; PDI = 1.03; degree of polymerization, n = 13.

P3-Me. It was synthesized using monomer **D3** (0.07 g, 0.077 mmol), monomer **7** (0.037 g, 0.077 mmol) and Pd(PPh$_3$)$_4$ (17.8 mg, 0.015 mmol). P3-Me was formed as red colored solid (55 mg, yield 79%). ^{1}H-NMR (600 MHz, CDCl$_3$, δ in ppm): 7.69-7.59

View Article Online
DOI: 10.1039/C8NJ05850D

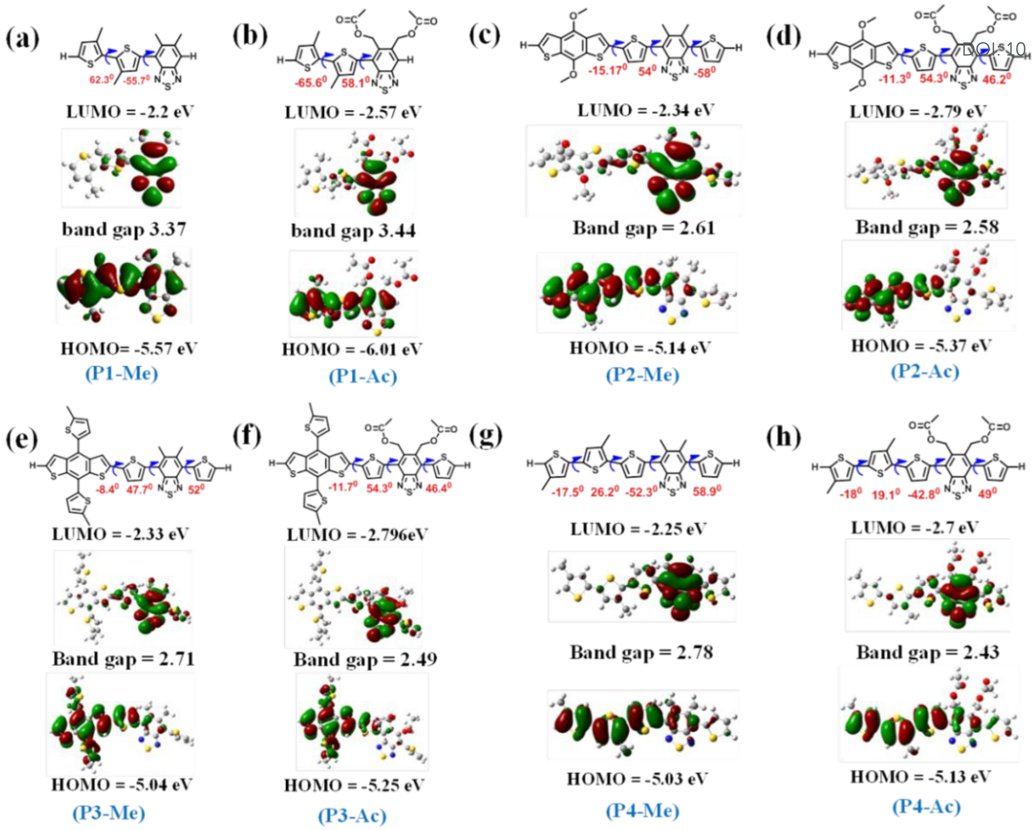

Fig. 3 DFT calculation showing lowering of LUMO on functionalization of methyl acetate at 5,6-positon of BT-based CPs (model is a monomer).

(br, 2H), 7.36-7.29 (br, 2H), 7.22-7.12 (br, 2H), 7.12-7.02 (br, 2H), 6.91-6.79b (br, 2H), 2.87-2.75 (br, 4H), 2.55-2.39 (br, 6H), 1.70-1.59 (br, 2H), 1.59-1.45 (br, 4H), 1.33-1.21 (br, 12H), 0.92-0.78 (br, 12H). ^{13}C-NMR (150 MHz, $CDCl_3$, δ in ppm): 153.45, 146.14, 139.91, 139.18, 138.77, 137.69, 137.37, 137.19, 136.83, 130.13, 129.32, 128.89, 127.87, 125.54, 125.29, 125.18, 124.04, 123.52, 121.19, 119.49, 114.11, 41.46, 34.33, 32.51, 28.95, 25.80, 23.07, 19.29, 14.23, 10.95. GPC: M_n = 11142 g/mol.; M_w = 13924 g/mol.; PDI = 1.24; degree of polymerization n = 12.

P3-Ac. It was synthesized using monomer **D3** (0.07 g, 0.077 mmol), monomer **9** (0.0466 g, 0.077 mmol) and $Pd(PPh_3)_4$ (17.8 mg, 0.015 mmol). P3-Ac was formed as deep red colored solid (60 mg, yield 76%). ^{1}H-NMR (600 MHz, $CDCl_3$, δ in ppm): 7.72-7.63 (br, 2H), 7.37-7.30 (br, 2H), 7.30-7.24 (br, 2H), 7.24-7.15 (br, 2H), 6.91-6.81 (br, 2H), 5.36-5.22 (br, 4H), 2.86-2.76 (br, 4H), 2.12-2.03 (br, 6H), 1.68-1.61 (br, 2H), 1.61-1.47 (br, 4H), 1.32-1.23 (br, 12H), 0.94-0.78 (br, 12H). ^{13}C-NMR (150 MHz, $CDCl_3$, δ in ppm): 170.14, 154.17, 146.14, 140.58, 139.28, 138.95, 138.12, 137.41, 136.71, 135.29, 135.17, 130.85, 130.15, 129.66, 127.94, 125.55, 125.34, 124.51, 123.68, 119.97, 115.54, 114.08, 61.98, 34.33, 32.53, 28.94, 25.77, 23.10, 20.98, 14.20, 10.95. GPC: M_n = 9937 g/mol.; M_w =10605 g/mol.; PDI = 1.06; degree of polymerization, n = 9.

P4-Me. It was synthesized using monomer **D4** (0.07 g, 0.0844 mmol), monomer **7** (0.0409 g, 0.0844 mmol) and $Pd(PPh_3)_4$ (19.5 mg, 0.0169 mmol). P4-Me was formed as deep red colored solid (53 mg, yield 76%). ^{1}H-NMR (600 MHz, $CDCl_3$, δ in ppm): 7.20-7.16 (br, 2H), 7.16-7.08 (br, 2H), 7.01-6.93 (br, 2H), 2.78-2.70 (br, 2H), 2.55-2.40 (br, 6H), 1.69-1.59 (br, 4H), 1.41-1.31 (br, 2H), 1.25-1.06 (br, 36H), 0.84-0.74 (br, 6H). ^{13}C-NMR (150 MHz, $CDCl_3$, δ in ppm): 153.60, 143.48, 140.45, 139.79, 138.62, 137.79, 137.01, 136.74, 134.97, 129.94, 129.52, 126.62, 125.39, 123.93, 114.02, 31.96, 31.94, 30.58, 29.70-29.38 (many peaks), 22.72, 19.24, 14.17. GPC: M_n = 15325. g/mol.; M_w = 17370 g/mol.; PDI = 1.33; degree of polymerization, n = 18.

P4-Ac. It was synthesized using monomer **D4** (0.06 g, 0.0724 mmol), monomer **9** (0.0436 g, 0.0724 mmol) and $Pd(PPh_3)_4$ (16.7 mg, 0.0144 mmol). P4-Ac was formed as deep red colored solid (59 mg, yield 87%). ^{1}H-NMR (600 MHz, $CDCl_3$, δ in ppm):7.27-7.15 (br, 4H), 7.04-6.93 (br, 2H), 5.37-5.27 (br, 4H), 2.80-2.69 (br, 2H), 2.14-2.04 (br, 6H), 1.69-1.61 (br, 4H), 1.40-1.32 (br, 2H) 1.25-1.06 (br, 36H), 0.84-0.74 (br, 6H). ^{13}C-NMR (150 MHz, $CDCl_3$, δ in ppm): 170.24, 154.28, 140.98, 139.31, 135.24, 135.0, 134.55, 130.88, 130.50, 129.72, 129.20, 129.0, 126.77, 125.62, 124.51, 114.08, 62.1, 31.94, 31.92, 30.58, 29.7-29.39 (many peaks), 22.65, 21.04, 14.20. GPC: M_n = 14008 g/mol.; M_w = 18199 g/mol.; PDI = 1.29; degree of polymerization, n = 14.

View Article Online
DOI: 10.1039/C8NJ05850D

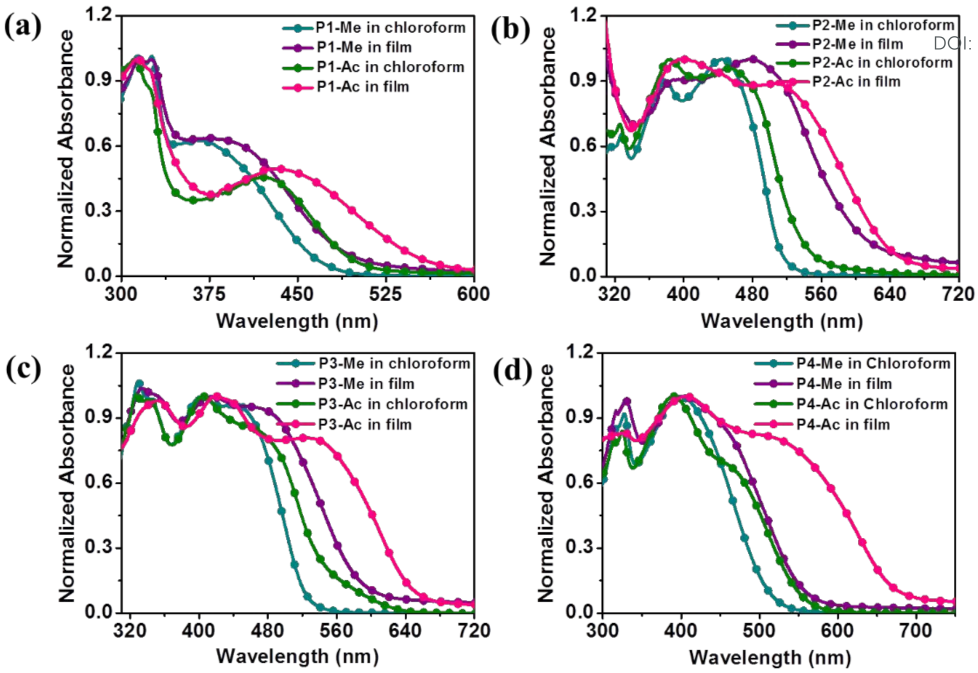

Fig. 4 Absorption spectra of synthesized CPs, showing red-shift and broadening of spectra for methyl acetate substituted CPs compared to their methyl counterpart.

Results and discussion

Theoretical calculations

Influence of ester group on HOMO-LUMO levels and dihedral angle between conjugated units of the polymers have been studied using DFT calculation at B3LYP/6-31G (*d,p*). For simplifying calculations, methyl chain have been used for any kind of alkyl chain and investigation on all CPs have been carried out taking 1 unit of each CP. Ester functionalised CPs displayed required distribution of charge density for intra-molecular charge transfer (ICT) from donor to acceptor (distribution of charge density all over HOMO and localization of charge density on acceptor only in LUMO)[46] in all four CPs [P(1,2,3,4)-Ac] with 4 different donors (D1 to D4). Ester functionalized CP has low dihedral angle in case of D2 and D4 compared to their methyl counterpart (Fig. 3c,d and 3g,h), due to possible oxygen (negatively charged in ester group)-sulphur (positively charges in thiophene ring) interactions. But in case of D1 and D3 dihedral angle increases in ester functionalized CPs (Fig. 3a,b and 3e,f) compared to its methyl counterpart because of steric hindrance caused by D1 with two dodecyl chains in close position (at 3,3´) and bulkiness of D3 (due to two thiophene substituted 2-ethylhexyl chain on BDT), which predominates over any possible oxygen sulphur interactions. In case of **D2** and **D4** dihedral angle reduced by 10° in ester substituted CP.

Optical properties

UV-visible spectra for both methyl acetate substituted CPs [P(1,2,3,4)-Ac] and methyl substituted CPs [P(1,2,3,4)-Me] at 5,6-position of BT have been recorded from dilute $CHCl_3$ solution and in film state (drop casted from chlorobenzene). A comparison of absorption property for both solution and film shows bathochromic shift of both absorption maximum of ICT transition and absorption onset with broadening of UV-visible spectra for ester functionalized CPs compared to their methyl counterpart (Table 1, Fig. 4a to 4d). All CPs exhibit tri-humped peak (Fig. 4a to 4d) in general both in solution and film state, which refers to high energy intrinsic band for donor only, moderate energy π-π^* transition for CP backbone and low energy ICT band.[47] In film state, intrinsic band for P1-Me, P1-Ac and P2-Me is not clearly visible due to broadening of spectra (Fig. 4a and 4b). In solution state, in addition to small variation in intrinsic band and π-π^* band, a red-shift in ICT transition has been observed for methyl acetate substituted CPs compared to their methyl counterpart. In film state a significant bathochromic shift of absorption spectra has been observed along with peak broadening for λ_{max} (ICT band) and/or UV-visible (onset), signifying a substantial π-π stacking of CP main chain (Fig. 4a to 4d),[48] when side chain ester was introduced into it, due to enhanced CH-π, π-π and oxygen-sulphur interaction (intramolecular and intermolecular). Molar absorption coefficient (ε) of π-π^* band and ICT band in $CHCl_3$ was higher for ester substituted CPs P2-Ac (27373, 26197 L mol^{-1} cm^{-1}) and P4-Ac (29827, 20113 L mol^{-1} cm^{-1}) compared to methyl substituted CP P2-Me (13820, 15372 L mol^{-1} cm^{-1}) and P4-Me (18124, 19819 L mol^{-1} cm^{-1}) respectively (Table 1), due to lowering of dihedral angle. However for similar instance, ester substituted CP P1-Ac and P3-Ac molar absorption coefficient gets lowered compared to their methyl counterpart P1-Me and P3-Me due to higher dihedral angle in ester substituted CPs caused due to steric hindered donor D1 (Fig. 2) with closely positioned dodecyl chain[1] in case of P1-Ac and

View Article Online
DOI: 10.1039/C8NJ05850D

Table 1 Optical properties and voltammetry for synthesized CPs with degradation temperature corresponding to 5% weight loss.

P	λ_{max} [nm]	λ_{onset} [nm]	λ_{max} film [nm]	λ_{onset} film [nm]	E_{ox} [Volt]	HOMO^{el} [eV]	LUMO^{opt} [eV]	ε (π-π*, ICT) [L mo^{-1} cm^{-1}]	T_{5D} [°C]
P1-Me	316, 326, 369	470	327, 374	490	+0.801	-5.49	-2.94	16757, 10282	368 ($T_{10\ D}$)
P1-Ac	312, 324, 421	496	326, 433	558	+0.92	-5.609	-3.32	16942, 8247	272
P2-Me	328, 379, 445	511	388, 480	602	+1.03	-5.39	-3.33	13820, 15372	275
P2-Ac	326, 382, 454	543	400, 515	644	+1.04	-5.40	-3.47	27373, 26197	244
P3-Me	329, 404, 440	526	333, 416, 462	586	+0.77	-5.49	-3.38	41536, 40772	275
P3-Ac	339, 404, ~470	555	352, 420, 523	648	+0.74	-5.46	-3.55	23934, 20532	265
P4-Me	327, 401,	510	330, 404, 460	557	+0.66	-5.38	-3.16	18124, 19819	348
P4-Ac	325, 390, ~457	554	327, 401, 512	670	+0.64	-5.36	-3.51	29827, 20113	279

bulky 2-ethylhexylthiophene substituted BDT-Th donor D3 (Fig. 2) in case of P3-Ac, which predominantly controls the structure, eliminating possible oxygen-sulphur interactions by ester group with near Th-units which could stabilize the structure.

Electrochemical properties

Cyclic voltammetry was carried out for all synthesized CPs and they exhibited only an oxidation potential within -0.6 Volt to -1.04 Volts (Fig. 5a and 5b). Calculated HOMO of all CPs is in the range from -5.36 to -5.6 eV. HOMO of P1-Ac is 0.11 eV deeper than P1-Me (Table 1), which might have caused due to high sterically hindered donor D1, leading to weak donating tendency to the acceptor BT having methyl acetate group (higher the π-electron donating tendency of donor in D-A CP, higher the HOMO). Minor fluctuation (maximum observed change 0.03 eV) of HOMO levels has been observed[49] in P2-Ac, P3-Ac and P4-Ac compared to their methyl counterpart, indicating less control of ester group on HOMO of synthesized CPs and influence of methyl acetate group on CP photo physical property purely due to contribution to LUMO only. None of the CPs exhibited a reduction potential, hence their LUMO^{optical} have been calculated from absorption onset using formula (band gap = λ_{onset}/1240 and LUMO^{opt} = HOMO + band gap). As all ester substituted CPs show a high absorption onset, hence all ester functionalized CPs showed a low LUMO^{opt} compared to its methyl counterpart. Low lying LUMO^{opt} in ester functionalized CPs will help improve charge separation in active layer of fabricated PSC due to small energy barrier between LUMO levels of CP and PC$_{71}$BM.[50]

Thermal stability of polymers

Thermal stability for all side chain ester and methyl functionalized CPs have been investigated using TGA analysis under nitrogen atmosphere. All CPs are stable up to 250 °C, corresponding to 5% weight loss of CP (Table 1, Fig. 6a and 6b) on a constant heating rate of 10 °C per minute, which is adequate temperature for device Fabrication.[51,52] With exception, sticky natured CP P1-Me starts degrading at less than 100 °C (Fig. 6a) corresponding to 5% weight loss and might have occurred due to the presence of moisture (which might have been responsible for its sticky nature). In Table 1 for P3, T_{10D} (degradation corresponding to 10% weight loss) was at 368 °C. All ester functionalized CPs have low T_{5D} and show bi-humped degradation pattern compared to their methyl counterpart (Fig. 6a and 6b), which might have occurred due to (fragile/thermocleavable nature of side chain ester group (here methyl acetate).[42]

Solar cell performance

Both methyl ester and methyl functionalized on BT-based CPs have been used with PC$_{71}$BM to fabricate PSC and similar device architecture (ITO/PEDOT:PSS/CP:PC$_{71}$BM (1:1)/LiF/Al)

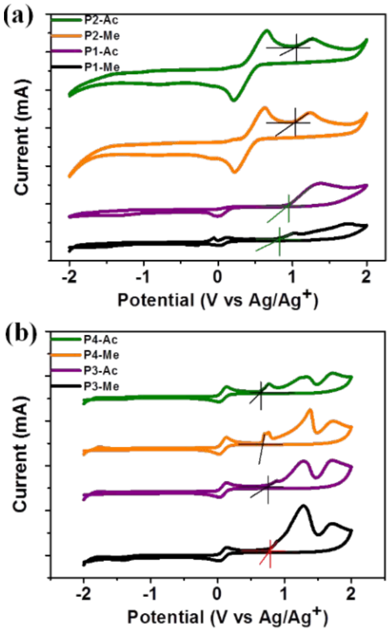

Fig. 5 CV for CPs, showing oxidation potential (a) P1-Me, P1-Ac, P2-Me, P2-Ac (b) P3-Me, P3-Ac, P4-AMe, P4-Ac.

View Article Online
DOI: 10.1039/C8NJ05850D

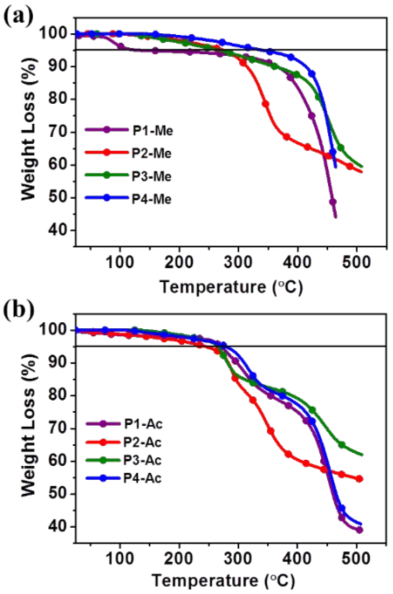

Fig. 6 TGA spectra for CPs showing T_{5D} (corresponding to 5% weight loss) (a) methyl substituted at 5,6-position of BT-based CPs (b) methyl acetate counterpart CP.

was chosen to establish the influence of side chain ester group on solar cell performance. It has been established that ester substituted CPs [P(2,3,4)-Ac] show high solar cell performance (PCE, V_{oc} and J_{sc}) than their methyl counterpart CP [P(2,3,4)-Me]]. With P2-Me:$PC_{71}BM$ (1:1) as active layer a PCE of 0.9% (J_{sc} = 5.09 mA/cm^2, V_{oc} = 0.68 V and FF = 26.2%) has been achieved, whereas ester functionalized CP P2-Ac in similar device configuration results in a PCE of 1.36% with J_{sc} of 7.4 mA/cm^2, V_{oc} of 0.69 V and FF of 26.5% (Table 2, Fig. 7a). Similarly with ester functionalized CP P3-Ac a PCE of 1.17% (J_{sc} = 7.65 mA/cm^2, V_{oc} = 0.63 V, FF = 29.3%) was achieved compared to a PCE of 0.54% (J_{sc} = 3.5 mA/cm^2, V_{oc} = 0.57 V, FF = 27.1%) for its methyl counterpart (P3-Me). Unexpected variation of V_{oc} with respect to HOMO for P3 set of polymers, might have resulted due to difference of side chain, from methyl (P3-Me) to acetate (P3-Ac). This dissimilarity of side chain changes the intermolecular interaction of polymer with $PC_{71}BM$[53,54] and affects the V_{oc} as well. PSC performance for P3-Ac has further improved to a PCE of 1.96% by the use of 3% 1,8-diiodooctane (DIO) as additive into active layer (Table 2, Fig. 7a).[24] The reason for improvement of PSC performance with DIO is mainly due to film reorganization and better phase separation (Fig. 8c).[55]

P4-Me and P4-Ac follow similar pattern as like P2-Me and P2-Ac in fabricated devices with PCE of 0.35% (P4-Ac) and 0.31% (P4-Me). Solar cell performance with P4-Me and P4-Ac (CP with DTh as donor) was very poor (PCE in the range of 0.3%) compared to BDT based CPs. This is due to poor film forming ability of P4-Me and P4-Ac with high dihedral angle (~18°) between two thiophene units (Fig. 3d) of the donor dithiophene (DTh), this leads to low rigidity of CP backbone and hence poor film forming property.[56] Moreover maximum external quantum efficiency of 37% (Fig. 7b) have been achieved with P3-Ac:$PC_{71}BM$ (1:1)-3% (DIO) as active layer for fabricated solar cells and improvement of EQE values have been observed subsequently with PCE in case of ester functionalized CPs compared to their methyl counterpart. This establishes side chain ester group at 5,6-position of BT improves solar cell performance, as studied in three different set of CPs with varying three donors (D2, D3, D4). In addition P1-Ac:$PC_{71}BM$ (2:1) showed a PCE of 0.02% (J_{sc} = 0.50 mA/cm^2, V_{oc} = 0.17 V and FF = 26.2%), which is too low to study any comparison with its methyl counterpart P1-Me. Both P1-Me and P1-Ac have very poor film forming property, due to high dihedral angle along the conjugation main chain.[57] The cause of improvement of solar cell performances in case of ester substituted CPs is due to higher absorption range (red-region), better phase separation in active layer due to cross linking nature of ester group within CP and/or $PC_{71}BM$, improved ICT

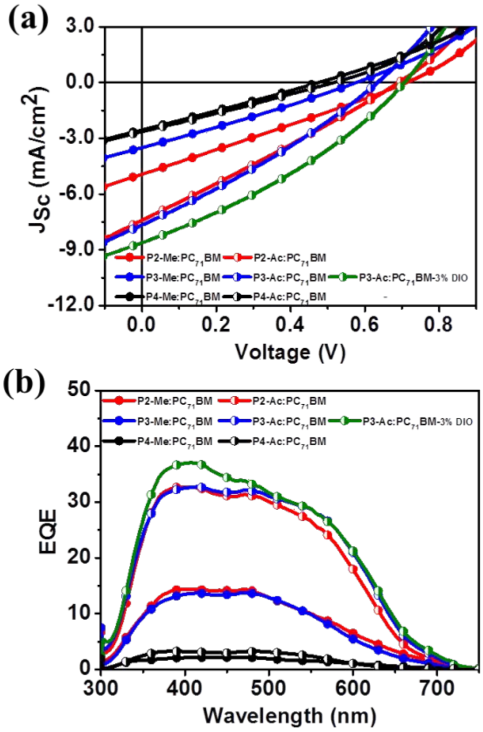

Fig. 7 Solar cell performance for side chain methyl acetate and methyl containing BT-based CPs (a) *J-V* curve (b) external quantum efficiency.

Table 2 Solar cell parameters for fabricated bulk-heterojunction devices.

Active layer[a]	V_{oc} [Volt]	J_{sc} [mA/cm^2]	FF [%]	Max PCE [%][b]
P2-Me	0.68	5.09	26.2	0.91 [0.86±0.09]
P2-Ac	0.69	7.40	26.5	1.36 [1.29±0.06]
P3-Me	0.57	3.50	27.1	0.55 [0.54±0.01]
P3-Ac	0.63	7.65	29.3	1.17 [1.13±0.05]
P3-Ac-3% DIO	0.70	8.62	32.3	1.96 [1.95±0.01]
P4-Me	0.47	2.54	26.3	0.31 [0.28±0.03]
P4-Ac	0.51	2.62	26.2	0.36 [0.32±0.05]

[a] active layer for each CP was CP:$PC_{71}BM$ (1:1), [b] Average PCE of three cell given in parenthesis.

View Article Online
DOI: 10.1039/C8NJ05850D

due to lowering in dihedral angle along conjugation main chain and lowering of LUMO which facilitates ease of separation of exciton from LUMO of CP to LUMO of $PC_{71}BM$.

Morphology of active layer of fabricated PSCs

Tapping mode AFM images have been recorded to investigate nano-morphology of active layer for fabricated devices by spin coating polymer:$PC_{71}BM$ blend on a pre-cleaned ITO coated glass slide. As compared for P3-Me:$PC_{71}BM$ (1:1), P3-Ac: $PC_{71}BM$ (1:1) and P3-Ac: $PC_{71}BM$ (1:1)with DIO, it was observed that both the polymer-$PC_{71}BM$ blend have proper miscibility in the active layer with RMS (root mean square) roughness less than 3 nm.[47] Ester functionalized polymer P3-Ac results in better phase separation between P3-Ac and $PC_{71}BM$ in the blend film compared to its methyl counterpart P3-Me (Fig. 8a and 8b). When 3% DIO was added into the P3-Ac:$PC_{71}BM$ (1:1) a significant improvement of phase separation[55,58] has been observed (Fig. 8c) allowing distinguished path for electron and hole to travel and reducing recombination of generated excitons (as can be seen in the height and 3D view of height images in Fig. 8). As a result PCE improved to 1.96% with P3-Ac:$PC_{71}BM$ (1:1)-3% DIO as active layer. This further confirms the positive influence of side chain ester group in gaining crtystallinity[59] in the active layer of fabricated PSC with tunability to external effects like additives and various solvent processing.

Thin film X-ray diffraction pattern

Thin film X-ray diffraction has been carried out by spin coating equal concentration of methyl and corresponding ester substituted CPs in order to investigate influence on π-π stacking distance in thin-film state with side chain ester substitution at 5,6-position of BT. For P4-Me and P4-Ac the diffraction peaks were observed at $2\theta = 24.21^{o}$ and 25.2^{o} which corresponds to 0.3673 nm and 0.3531 nm π-π stacking distance respectively (Fig. S1c, †ESI). Close π-π stacking distance in case of ester substituted CP P4-Ac compared to P4-Me further confirms improved π-π stacking within CP chain in film state and hence better solar cell performance.[10,60] In addition among P3-Me and P3-Ac, ester substituted at 5,6-position of BT CP P3-Ac exhibited a similar/small increase in π-π stacking distance ($2\theta = 23.16^{o}$, π-π stacking distance = 0.3837 nm) as obvious due to small increase in dihedral angle (Fig. S1b, †ESI) (determined by DFT) compared to its methyl counterpart P3-Me ($2\theta = 23.25^{o}$, π-π stacking distance = 0.3822 nm). Similarly in case of P2-Me and P2-Ac no change in π-π distance was observed (Fig. S1a, †ESI). DTh and BDT-Th) resulting in new CPs–having methyl acetate group at 5,6-location of BT. All newly synthesized methyl and methyl acetate substituted 5,6-BT-based CPs were well soluble in commonly used solvent for device fabrication (CB, DCB $CHCl_3$, THF) and additionally the ester substituted CPs are stable up to 250 °C. With this study it has been established that functionalizing ester group at 5,6-position of BT, reduces the dihedral angle in the CP backbone due to oxygen-sulphur interaction, improves π-π stacking in film leading to red-shift and broadening of absorption spectra, lowers $\text{LUMO}^{\text{optical}}$ for CP, improves phase separation of active layer of fabricated

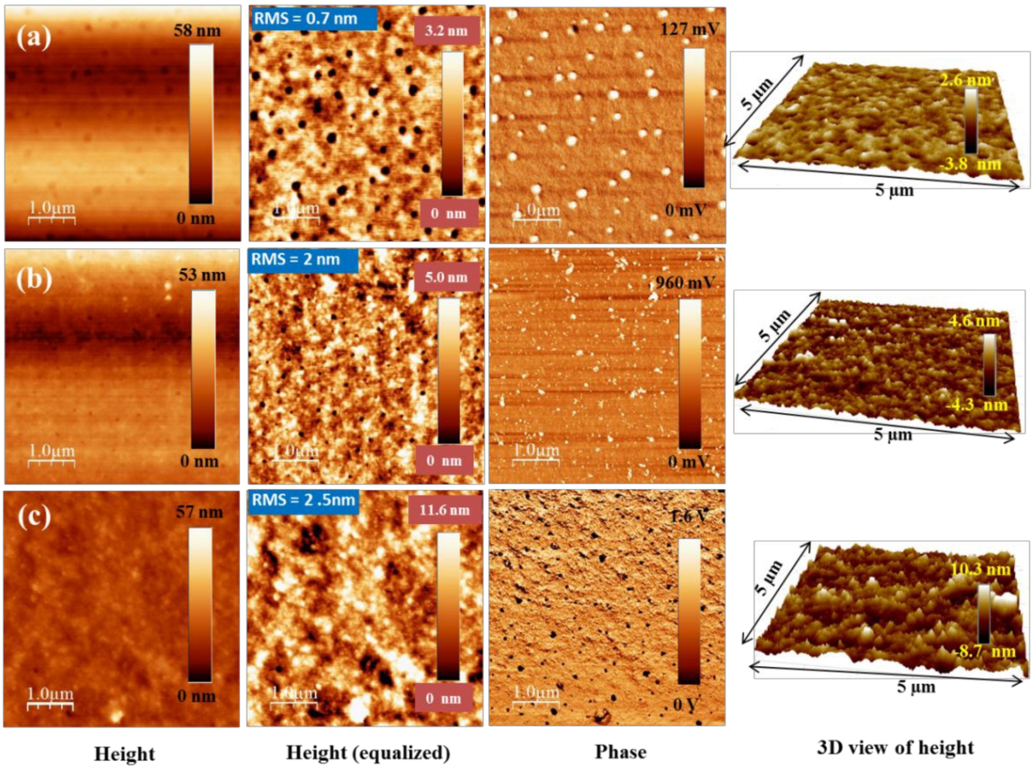

Fig. 8 Morphology of active layer (CP:$PC_{71}BM$ blend) of fabricated PSCs show improvement of phase separation with ester substituted CPs and the phase separation further improved to large extent when 3% DIO was added to P3-Ac:$PC_{71}BM$ (1:1). (a) P3-Me:$PC_{71}BM$ (1:1) (b) P3-Ac:$PC_{71}BM$ (1:1) (c) P3-Ac:$PC_{71}BM$ (1:1)-3% DIO.

View Article Online
DOI: 10.1039/C8NJ05850D

solar cell and hence improves solar cell performance compared to methyl counterpart. This phase separation can be further enhanced using additives, as in case of P3-Ac:PC_{71}BM, PCE of 1.17% was improved to 1.96% by addition of 3% DIO as additive. Such side chain ester group with good photo-physical and morphological influence on CP film state can be introduced into side chain of synthetically feasible conjugated units and used to synthesize CP with superior properties for solar cells and other optoelectronic devices.

Acknowledgements

Authors acknowledge the Department of Science and Technology INDIA (No. SR/S1/PC-02/2009, DST/TSG/PT/2009/11 and DST/TSG/PT/2009/23), DST–Max Planck Society, Germany (IGSTC/MPG/PG(PKI)/2011A/48), Department of Electronics & Information Technology, (Deity) No. 5(9)/2012-NANO (Vol. II) for financial assistance. RR thanks UGC-INDIA for financial support. The Central Instruments Facility and Department of Chemistry, IIT Guwahati, are acknowledged for instrument facility. Sophisticated Analytical Instrumentation Centre, Tezpur University is acknowledged for GPC facility. Department of Chemistry, Guwahati University is acknowledged for NMR facility as well.

References

1 D. Liu, B. Yang, B. Jang, B. Xu, S. Zhang, C. He, H. Y. Woo, J. Hou, *Energy Environ. Sci*., 2017, **10,** 546-551.
2 N. Zhou, X. Guo, R. P. Ortiz, S. Li, S. Zhang, R. P. H. Chang, A. Facchetti, T. J. Marks, *Adv. Mater*., 2012, **24,** 2242-2248.
3 G. Zhang, K. Zhang, Q. Yin, X. F. Jiang, Z. Wang, J. Xin, W. Ma, H. Yan, F. Huang, Y. Cao, *J. Am. Chem. Soc*., 2017, **139**, 2387-2395.
4 N. Gasparini, X. Jiao, T. Heumueller, D. Baran, G. J. Matt, S. Fladischer, E. Spiecker, H. Ade, C. J. Brabec, T. Ameri, *Nat. Energy*., 2016, **1**, 16118.
5 Z. Hu, F. Zhang, Q. An, M. Zhang, X. Ma, J. Wang, J. Zhang, J. Wang, *ACS Energy Lett.*, 2018, **3**, 555-561.
6 J. You, L. Dou, K. Yoshimura, T. Kato, K. Ohya, T. Moriarty, K. Emery, C. C. Chen, J. Gao, G. Li, Y. Yang, *Nat. Commun*., 2013, **4**, 1446.
7 W. Zhao, S. Li, H. Yao, S. Zhang, Y. Zhang, B. Yang, J. Hou, *J. Am. Chem. Soc*., 2017, **139**, 7148-7151.
8 I. E. Kuznetsov, A. V. Akkuratow, D. K. Susarova, D. V. Anokhin, Y. L. Moskvin, M. V. Kluyev, A. S. Peregudov, P. A. Roshin, *Chem. Commun*., 2015, **51,** 7562-7564.
9 Y. J. Hwang, B. A. E. Courtright, A. S. Ferreira, S. H. Tolbert, S. A. Jenekhe, *Adv. Mater*., 2015, **27**, 4578-4584.
10 C. Cui, Z. He, Y. Wu, X. Cheng, H. Wu, Y. Li, Y. Cao, W. Y. Wong, *Energy Environ. Sci*., 2016, **9**, 885-891.
11 X. Wang, Y. Sun, S. Chen, X. Guo, M. Zhang, X. Li, Y. Li, H. Wang, *Macromolecules*, 2012, **45**, 1208-1216.
12 C. Gu, W. Dong, L. Yao, Y. Lv, Z. Zhang, D. Lu, Y. Ma, *Adv. Mater*., 2012, **24**, 2413-2417.
13 B. Meng, Y. Fu, Z. Xie, J. Liu, L. Wang, *Macromolecules*, 2014, **47**, 6246–6251.
14 J. Sun, Y. Zhu, X. Xu, L. Lan, L. Zhang, P. Cai, J. Chen, J. Peng, Y. Cao, *J. Phys. Chem. C*, 2012, **116**, 14188-14198.
15 N. Cho, C. W. Schlenker, K. M. Knesting, P. Koelsch, H. L. Yip, D. S. Ginger, A. K. Y. Jen, *Adv. Energy Mater*., 2014, 1301857.
16 H. J. Kim, A. R. Han, C. H. Cho, H. Kang, H. H. Cho, M. Y. Lee, J. M. J. Fréchet, J. H. Oh, B. J. Kim, *Chem. Mater*., 2012, **24**, 215-221.
17 Y. L, J. Zou, H. L. Yip, C. Z. Li, Y. Zhang, C. C. Chueh, J. Intemann, Y. Xu, P. W. Liang, Y. Chen, A. K. Y. Jen, *Macromolecules*, 2013, **46**, 5497-5503.
18 R. N. Brookins, E. Berda, J. R. Reynolds, *J. Mater. Chem*., 2009, **19**, 4197-4204.
19 F. S. U. Fischer, K. Tremel, A. K. Saur, S. Link, N. Kayunkid, M. Brinkmann, D. H. Carvajal, J. T. L. Navarrete, M. C. R. Delgado, S. Ludwigs, *Macromolecules*, 2013, **46**, 4924-4931.
20 D. D. Nuzzo, A. Aguirre, M. Shahid, V. S. Gevaerts, S. C. J. Meskers, R. A. J. Janssen, *Adv. Mater*., 2010, **22**, 4321-4324.
21 L. M. Chen, Z. Hong, G. Li, Y. Yang, *Adv. Mater*., 2009, **21**, 1434-1449.
22 F. Liu, Y. Gu, J. W. Jung, W. H. Jo, T. P. Russell, *J. Polym. Sci., Part A: Polym. Chem*., 2012, **50**, 1018-1044.
23 E. Wang, L. Hou, Z. Wang, S. Hellström, F. Z. O. Inganäs, M. R. Andersson, *Adv. Mater*., 2010, **22**, 5240-5244.
24 Y. Liang, Z. Xu, J. Xia, S. T. Tsai, Y. Wu, G. Li, C. Ray, L. Yu, *Adv. Mater*., 2010, **22,** E135-E138.
25 C. V. Hoven, X. D. Dang, R. C. Coffin, J. Peet, T. Q. Nguyen, G. C. Bazan, *Adv. Mater.*, 2010, **22**, E63-E66.
26 W. Cai, P. Liu, Y. Jin, Q. Xue, F. Liu, T. P. Russell, F. Huang, H. L. Yip, Y. Cao, *Adv. Sci*., 2015, **2**, 1500095.
27 J. Hou, H. Y. Chen, S. Zhang, Y. Yang, *J. Phys. Chem. C*, 2009, **113**, 21202-21207.
28 M. Zhang, F. Zhang, Q. An, Q. Sun, W. Wang, X. Ma, J. Zhang, W. Tang, *J. Mater. Chem. A*, 2017, **5**, 3589-3598.
29 J. W. Jo, S. Bae, F. Liu, T. P. Russell, W. H. Jo, *Adv. Funct. Mater*., 2015, **25**, 120-125.
30 N. Wang, Z. Chen, W. Wei, Z. Jiang, *J. Am. Chem. Soc*., 2013, **135**, 17060-17068.
31 Y. Liang, D. Feng, Y. Wu, S. T. Tsai, G. Li, C. Ray, L. Yu, *J. Am. Chem. Soc*., 2009, **131**, 7792-7799.
32 A. Li, J. Amonoo, B. Huang, P. K. Goldberg, A. J. McNeil, P. F. Green, *Adv. Funct. Mater*., 2014, **24**, 5594-5602.
33 S. Shi, Q. Liao, Y. Tang, H. Guo, X. Zhou, Y. Wang, T. Yang, Y. Liang, X. Cheng, F. Liu, X. Guo, *Adv. Mater*., 2016, **28**, 9969-9977.
34 D. Ouyang, M. Xiao, D. Zhu, W. Zhu, Z. Du, N. Wang, Y. Zhou, X. Bao, R. Yang, *Poly. Chem*., 2015, **6**, 55-63.
35 J. Hou, H. Y. Chen, S. Zhang, R. I. Chen, Y. Yang, Y. Wu, G. Li, *J. Am. Chem. Soc.*, 2009, **131**, 15586-15587.
36 B. Xia, K. Lu, L. Yuan, J. Zhang, L. Zhu, X. Zhu, D. Deng, H. Li, Z. Wei, *Poly. Chem*., 2016, **7**, 1323-1329.
37 X. Guo, N. Zhou, S. J. Lou, J. Smith, D. B. Tice, J. W. Hennek, R. P. Ortiz, J. T. L. Navarrete, S. Li, J. Strzalka, L. X. Chen, R. P. H. Chang, A. Facchetti, T. J. Marks, *Nat. Photonics*, 2013, **7**, 825-833.
38 C. Duan, J. J. V. Franeker, M. M. Wienk, R. A. J. Janssen, *Poly. Chem*., 2016, **7**, 5730-5738.
39 J. H. Dou, Y. Q. Zheng, Z. F. Yao, T. Lei, X. Shen, X. Y. Luo, Z. A. Yu, S. D. Zhang, G. Han, Z. Wang, Y. Yi, J. Y. Wang, J. Pei, *Adv. Mater*., 2015, **27**, 8051-8055.
40 J. Kesters, S. Kudret, S. Bertho, N. V. D. Brande, M. Defour, B. V. Mele, H. Penxten, L. Lutsen, J. Manca, D. Vanderzande, W. Maes, *Org. Electron*., 2014, **15**, 549-562.
41 J. Kesters, P. Verstappen, J. Raymakers, W. Vanormelingen, J. Drijkoningen, J. D'Haen, J. Manca, L. Lutsen, D. Vanderzande, W. Maes, *Chem. Mater*., 2015, **27**, 332-1341.
42 M. Helgesen, S. A. Gevorgyan, F. C. Krebs, R. A. J. Janssen, *Chem. Mater*., 2019, **21**, 4669-4675.

View Article Online
DOI: 10.1039/C8NJ05850D

43 Y. He, C. Guo, B. Sun, J. Quinn, Y. Li, *Poly. Chem.*, 2015, **6**, 6689-6697.

44 J. Y. Kim, Y. U. Kim, H. J. Kim, H. A. Um, J. Shin, M. J. Cho, D. H. Choi, *Macromol. Res.*, 2016, **24**, 980-985.

45 R. Ratha, A. Singh, T. B. Raju, P. K. Iyer, *Poly. Bull.*, DOI 10.1007/s00289-017-2193-x.

46 C. Y. Mei, L. Liang, F. G. Zhao, J. T. Wang, L. F. Yu, Y. X. Li, W. S. Li, *Macromolecules*, 2013, **46**, 7920-7931.

47 Y. Li, Y. Chen, X. Liu, Z. Wang, X. Yang, Y. Tu, X. Zhu, *Macromolecules*, 2011, **44**, 6370-6381.

48 X. Wang, S. Chen, Y. Sun, M. Zhang, Y. Li, X. Li, H. Wang, *Poly. Chem.*, 2011, **2**, 2872-2877.

49 H. Y. Chen, J. Hou, S. Zhang, Y. Liang, G. Yang, Y. Yang, L. Yu, Y. Wu, G. Li, *Nat. Photonics*, 2009, **3**, 649-653.

50 T. L. Nguyen, H. Choi, S. J. Ko, T. Kim, M. A. Uddin, S. Hwang, J. Y. Kim, H. Y. Woo, *Poly. J.*, 2017, **49**, 141-148.

51 L. Chen, P. Shen, Z. G. Zhang, Y. Li, *J. Mater. Chem. A*, 2015, **3**, 12005-12015.

52 C. H. Lee, Y. Y. Lai, F. Y. Cao, J. Y. Hsu, Z. L. Lin, U. S. Jeng, C. J. Su, Y. J. Cheng, *J. Mater. Chem. C*, 2016, **4**, 11427-11435.

53 Y. Li, J. Wang, Y. Liu, M. Qiu, S. Wen, X. Bao, N. Wang, M. Sun, R. Yang, *ACS Appl. Mater. Interfaces,* 2016, **8**, 26152-26161.

54 C. Cabanetos, A. E. Labban, J. A. Bartelt, J. D. Douglas, W. R. Mateker, J. M. J. Fré chet, M. D. McGehee, P. M. Beaujuge, *J. Am. Chem. Soc.*, 2013, **135**, 4656-4659.

55 S. Li, Z. Yuan, J. Yuan, P. Deng, Q. Zhang, B. Sun, *J. Mater. Chem. A*, 2014, **2**, 5427-5433.

56 J. M. Jiang, P. A. Yang, T. H. Hsieh, K. H. Wei, *Macromolecules*, 2011, **44**, 9155-9163.

57 H. Zhou, L. Yang, S. Xiao, S. Liu, W. You, *Macromolecules*, 2010, **43**, 811-820.

58 D. Liu, W. Zhao, S. Zhang, L. Ye, Z. Zheng, Y. Cui, Y. Chen, J. Hou, *Macromolecules*, 2015, **48**, 5172-5178.

59 S. Wakim, S. Alem, Z. Li, Y. Zhang, S. C. Tse, J. Lu, J. Ding, Y. Tao, *J. Mater. Chem.*, 2011, **21**, 10920-10928.

60 H. Kim, H. Lee, D. Seo, Y. Jeong, K. Cho, J. Lee, Y. Lee, *Chem. Mater.*, 2015, **27**, 3102-3107.

View Article Online
DOI: 10.1039/C8NJ05850D

Graphical Abstract

Substituting non-conjugating ester group on benzothiadiazole side chain in donor-acceptor polymer improves the solar cell performance

Radhakrishna Ratha[1], Mohammad Adil Afroz[2], Ritesh Kant Gupta[1] and Parameswar Krishnan Iyer *[1, 2]

[1]Centre for Nanotechnology and [2]Department of Chemistry, Indian Institute of Technology Guwahati, Guwahati-781039, Assam, INDIA

Text for graphical abstract:

Side chain ester substitution on donor-acceptor based conjugated polymers used as solar harvester in bulk-heterojunction (BHJ) polymer solar cell (PSC) can further improve harvesting property, phase separation in active layer and PSC performance.

Graphical abstract figure:

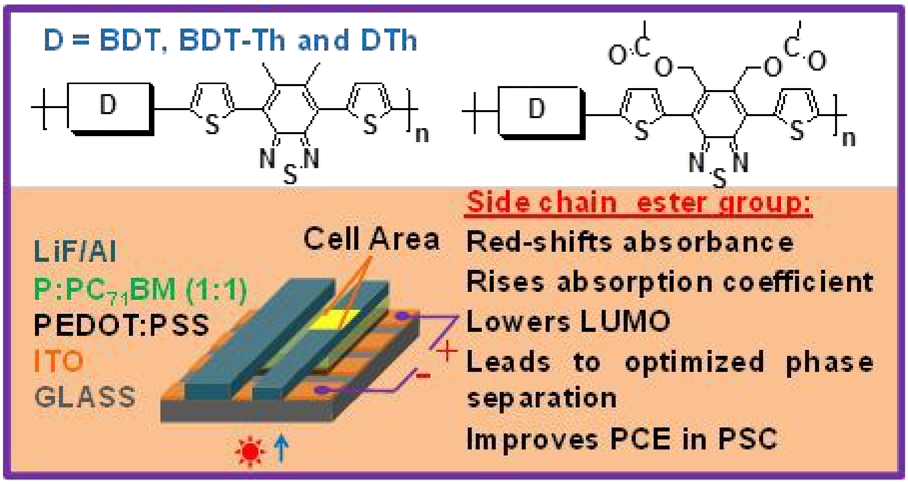

Figure: Graphical abstract.